JOC The Journal of Organic Chemistry
Cite This: J. Org. Chem. XXXX, XXX, XXX−XXX
Article
pubs.acs.org/joc

Ganolearic Acid A, a Hexanorlanostane Triterpenoid with a 3/5/6/5-Fused Tetracyclic Skeleton from *Ganoderma cochlear*

Xing-Rong Peng,[†] Yan-Jie Huang,[†,‡] Shuang-Yang Lu,[†,‡] Jing Yang,[†] and Ming-Hua Qiu*[,†,‡]

[†]Key Laboratory of Phytochemistry and Plant Resources in West China, Kunming Institute of Botany, Chinese Academy of Sciences, Kunming 650201, People's Republic of China

[‡]Graduate University of the Chinese Academy of Sciences, Beijing 100049, People's Republic of China

Supporting Information

ABSTRACT: Ganolearic acid A (**1**), a 3,4-*seco*-hexanortriterpenoid featuring a rare 3/5/6/5 tetracyclic system, was obtained in trace amounts from *Ganoderma cochlear* by a LC-UV/MS-guided method. Meanwhile, a new 3,4-*seco*-nortriterpenoid, fornicatin M (**2**), as well as its biogenetic precursor, fornicatin D (**3**), was isolated. The stereochemical structure of **1** was completely established by 1D, 2D NMR, IR, and HRMS spectra, as well as ^{13}C NMR and electronic circular dichroism calculations. The plausible biogenetic pathway of **1** and **2** was proposed. Furthermore, their anti-inflammatory activities were evaluated.

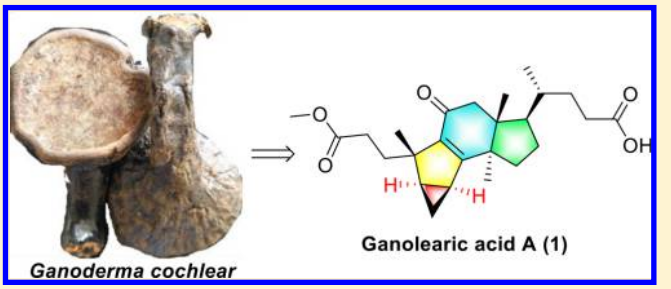

INTRODUCTION

Since the first *Ganoderma* triterpenoids (GTs) were isolated from *Ganoderma lucidum* in 1982,[1] GTs have been a research focus. GTs are a class of structurally diverse lanostane-type triterpenoids with a wide range of bioactivities.[2−6] On the basis of the number of carbon atoms, GTs can be divided into six subtypes, including C31, C30, C29, C27, C25, and C24.[7] Because of the diverse enzyme system in *Ganoderma*, many novel rearranged triterpenoids have been discovered, such as ganorbiformin A with a 15-methyl fragment,[8] cochlates A and B having a 3,4-*seco*-9,10-*seco*-9,19-cyclo skeleton,[9] and ganosinensic acid A possessing a 1,11-cyclo four-membered carbon ring motif.[10]

To simply, rapidly, and directly isolate new GTs from the genus *Ganoderma*, a structure-guided isolation approach was used on the basis of our long-established GTs library. By using this approach, we rapidly gained a series of new GTs from *G. cochlear*, including a hexanorlanostane triterpenoid with a five-membered carbon ring connecting to a γ-lactone ring through a carbon bond, three 3,4-*seco*-nortriterpenoids, and eight new lanostane triterpenoids.[11] Analysis of the GT library indicated that the molecular weight ranged from 350 to 600.[7] Meanwhile, the HPLC profile of the GTs showed most of the peaks with a maximum UV absorption band at 210−270 nm, indicating the existence of the double bond and α,β-unsaturated carbonyl or conjugated double bonds. Therefore, if the different maximum UV absorption wavelength is detected, it allows us to assume that the structure may have changed. It is worth mentioning that a minor GT (2.5 mg) featuring a 3/5/6/5 tetracyclic system with a λ_{max} at 285 nm, named ganolearic acid A (**1**), was isolated from *G. cochlear* using a LC-UV/MS screening approach. Meanwhile, its biogenetic analogue, fornicatin M (**2**), and a known compound, fornicatin D (**3**) (Figure 1), were gained. Herein, we reported their isolation, structural elucidation, and anti-inflammatory activity.

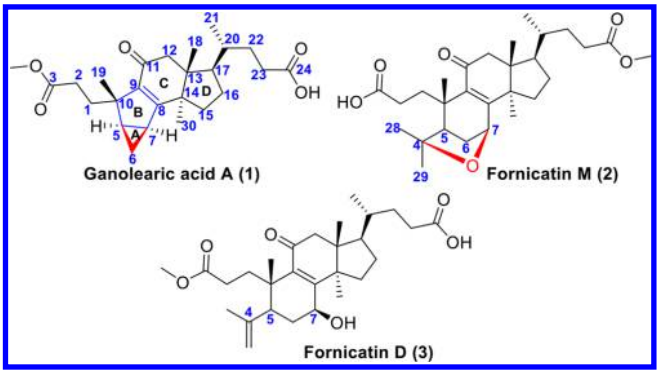

Figure 1. Structures of compounds **1**−**3** from *G. cochlear*.

RESULTS AND DISCUSSION

Ganoderma cochlear (32 kg) was extracted with 95% EtOH under reflux. Then the residue was suspended in H_2O and extracted with EtOAc, which was treated by a series of column chromatographic methods. Different polar fractions were analyzed by UPLC-MS-IT-TOF (Figure S1). Finally, ganolearic acid A (**1**, 2.5 mg, t_R = 21.5 min) with a λ_{max} at 285 nm was purified by HPLC on a RP-18 column (CH_3CN/H_2O + 0.1%

Received: July 25, 2018

DOI: 10.1021/acs.joc.8b01906
J. Org. Chem. XXXX, XXX, XXX−XXX

Table 1. ^{1}H and ^{13}C NMR Spectroscopic Data (δ in ppm) of Compounds 1 and 2

	1[a]		1[b]		2[a]	
position	^{1}H (J)	^{13}C	^{1}H (J)	^{13}C	δ_H (J in Hz)	δ_C
1	1.45, m; 1.96, m	36.0 CH_2	1.73, m; 2.15, m	36.7 CH_2	3.02, m; 2.19, m	37.7 CH_2
2	2.25, m; 2.45, m	29.6 CH_2	2.09, m; 2.34, m	30.3 CH_2	2.63, m	29.9 CH_2
3		174.2 C		176.3 C		174.4 C
4						84.4 C
5	1.47, m	27.8 CH	1.57, m	29.1 CH	2.03, m	51.9 CH
6	0.20, m; 0.87, m	14.5 CH_2	0.28, m; 1.05, m	15.3 CH_2	2.15, m; 1.27, m	32.4 CH_2
7	1.79, m	22.9 CH	1.98, m	24.1 CH	4.22, d (2.8)	73.1 CH
8		175.9 C		180.3 C		161.0 C
9		132.8 C		133.8 C		134.5 C
10		48.6 C		49.7 C		41.3 C
11		196.3 C		199.5 C		199.5 C
12	2.45, d (16.0); 2.61, d (16.0)	49.7 CH_2	2.60, d (17.6); 2.29, d (17.6)	50.6 CH_2	2.63, d (17.8); 2.54, d (17.8)	50.6 CH_2
13		48.0 C		48.8 C		45.1 C
14		50.1 C		51.5 C		50.6 C
15	1.38, m; 1.70, m	29.6 CH_2	1.59, m; 1.87, m	30.5 CH_2	1.91, m; 1.30, m	29.3 CH_2
16	2.00, m	27.5 CH_2	1.54, m; 2.14, m	28.4 CH_2	1.87, m	26.8 CH_2
17	1.71, m	49.5 CH	1.84, m	50.5 CH	1.58, m	49.8 CH
18	0.70, s	17.3 CH_3	0.79, s	17.8 CH_3	0.95, s	17.7 CH_3
19	1.40, s	23.0 CH_3	1.25, s	23.3 CH_3	1.58, s	25.3 CH_3
20	1.44, m	35.9 CH	1.49, m	37.0 CH	1.33, m	35.8 CH
21	0.82, d (5.8)	17.9 CH_3	0.91, d (6.5)	18.4 CH_3	0.76, d (6.1)	17.6 CH_3
22	1.45, m; 2.01, m	31.5 CH_2	2.24, m; 2.36, m	32.2 CH_2	2.36, m; 2.23, m	31.0 CH_2
23	2.43, m; 2.57, m	31.7 CH_2	1.84, m; 1.33, m	32.0 CH_2	2.16, m; 1.80, m	31.0 CH_2
24		176.2 C		177.9 C		174.0 C
28					1.46, s	29.0 CH_3
29					1.27, s	33.2 CH_3
30	1.10, s	24.5 CH_3	1.21, s	25.0 CH_3	0.85, s	24.3 CH_3
OCH_3	3.59, s	51.1 CH_3	3.61, s	52.0 CH_3	3.63, s	51.3 CH_3

[a]Measured in C_5D_5N (600/150 MHz). [b]Measured in CD_3OD (800/200 MHz).

trifluoroacetic acid = 48:52, flow rate = 3 mL/min) (Figure S1).

The molecular formula of ganolearic acid A (**1**) was assigned as $C_{25}H_{36}O_5$ by HRESIMS ($[M - H]^-$, m/z 415.2491; calcd 415.2490) with eight indices of hydrogen deficiency. The presence of hydroxyl, α,β-unsaturated carbonyl, and ester carbonyl groups was proven by its IR absorption bands at 3433, 1683, and 1638 cm^{-1}. The ^{1}H NMR spectrum (Table 1) of **1** displayed three singlet methyls (δ_H 1.40, H_3-19; δ_H 1.10, H_3-30; δ_H 0.70, H_3-18), one doublet methyl (δ_H 0.82, d, J = 5.8 Hz, H_3-21), one methoxy (δ_H 3.59, s), eight methylenes, and four methines. In the ^{13}C NMR spectrum of **1**, one carboxyl signal at δ_C 176.2 (C-24), one ester canbonyl signal at δ_C 174.2 (C-3), and the characteristic signals at δ_C 175.9 (C-8), δ_C 132.8 (C-9) and δ_C 196.3 (C-11) for an α,β-unsaturated ketone carbonyl fraction were observed. Except for the above functionalities, four rings were present in **1** due to the remaining four degrees of unsaturation, which hinted that **1** was highly degraded lanostane-type triterpenoids. By analyzing HMBC, HSQC, and $^{1}H-^{1}H$ COSY correlations (Figure 2), we found the C and D rings (Figure 1) and side chain of **1** were the same as those of fornicatin D (**3**).[11]

Furthermore, the HMBC spectrum of **1** showed long-range correlations (Figure 2) of H_3-19 to C-9, C-1, C-10, and C-5; of H_2-1 to C-2, C-3 (δ_C 174.2), C-9, C-10, and C-5; of H_2-2 to C-1, C-3, and C-10; of OCH_3 to C-3, suggesting that compound **1** was a 3,4-*seco*-nortriterpenoid and the methoxyl was located at C-3. Detailed analysis of the HMBC spectrum showed that both H-5 and H-7 correlated with C-8, C-9, and C-10.

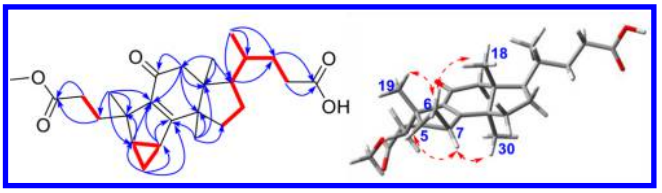

Figure 2. Selected HMBC (H → C), $^{1}H-^{1}H$ COSY (—), and ROESY (↔) correlations of **1**.

Together, the $^{1}H-^{1}H$ COSY correlation between H-5 and H-7 indicated the presence of a five-membered carbon ring (B ring, Figure 1), which also led to the low field chemical shift of C-8 (δ_C 175.9). Interestingly, H-5 and H-7 also showed $^{1}H-^{1}H$ COSY correlations with H-6. Additionally, H-6 correlated with C-5, C-10, C-7, and C-8 in the HMBC spectrum of **1**. This information allowed us to unambiguously deduce the presence of a three-membered carbon ring (A ring, Figure 1), which corresponded well with the diagnostic hydrogen signals of H_2-6 (δ_H 0.20, m; δ_H 0.87, m).[12−14]

Considering biogenesis of GTs, the absolute configurations of C-13, C-14, C-17, and C-20 are *R*, *R*, *R*, and *R*, respectively, which are characteristics of all lanostane-type triterpenoid derivatives isolated to date.[15−17] The ROESY correlations of H-5/H-7/H_3-30 and H_3-19/H-6 (δ_H 0.20)/H_3-18 indicated that H-5, H-7, and H_3-30 were cofacial, whereas H-6 (δ_H 0.20), H_3-18, and H_3-19 were on the same side. Thus, the absolute configurations of C-5, C-7, and C-10 could be *R*, *S*, *S* or *S*, *R*,

DOI: 10.1021/acs.joc.8b01906
J. Org. Chem. XXXX, XXX, XXX−XXX

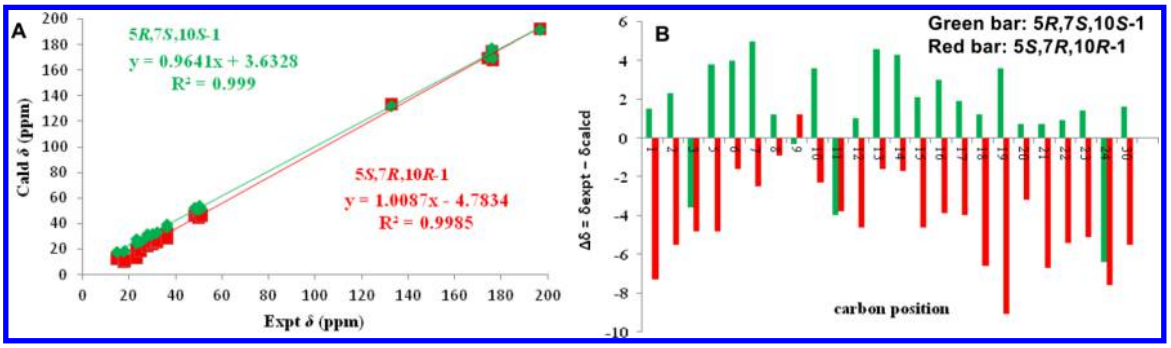

Figure 3. (A) Regression analysis of experimental versus calculated ^{13}C NMR chemical shifts of 5*R*,7*S*,10*S*-**1** and 5*S*,7*R*,10*R*-**1**, with linear fitting shown as a line. (B) Relative chemical shift errors between calculated and experimental ^{13}C NMR data for 5*R*,7*S*,10*S*-**1** and 5*S*,7*R*,10*R*-**1** (δ_{corr} obtained by linear fit δ_{expt} versus δ_{calcd}).

R. The computational methods were carried out to confirm the absolute configuration of **1**.

The selected conformations were optimized using the B3LYP/6-31G(d,p) method.[18] The calculated ^{13}C NMR chemical shifts were analyzed by subtracting the isotopic shifts for TMS calculated with the same methods.[18] Different conformers for 5*R*,7*S*,10*S*-**1** and 5*S*,7*R*,10*R*-**1** were considered. In the different conformers, the average values of the same atoms were calculated.[19] Differences ($\Delta\delta$) were determined according to the formula $\Delta\delta = \delta_{calcd} - \delta_{exptl}$, and the results are shown in Tables S3 and S6. The correlation coefficient (R^2) obtained by linear regression analysis, the mean absolute deviation (MAD), and largest absolute deviation (LAD) for 5*R*,7*S*,10*S*-**1** were 0.999 (Figure 3A), 2.59, and 6.4 (Figure 3B), whereas R^2, MAD, and LAD values for 5*S*,7*R*,10*R*-**1** were 0.9985, 9.1, and 4.37, respectively, which supported C-5, C-7, and C-10 to be *R*, *S*, and *S* configurations, respectively.

Subsequently, the theoretical calculation of ECD was performed,[20] and the calculated ECD curve of 5*R*,7*S*,10*S*-**1** was identical to the experimental ECD curve (Figure 4). Hence, the ECD calculation further confirmed the stereochemistry of **1** and ensured the rationality of the carbon skeleton of **1**.

Fornicatin M (**2**) was isolated as a white powder, and its molecular formula was determined to be $C_{28}H_{42}O_6$ on the basis of the HRESIMS and ^{13}C-DEPT NMR spectra of **2**, indicating eight indices of hydrogen dificiency. Meanwhile, its UV, IR, and 1D NMR spectra showed similarities with those of

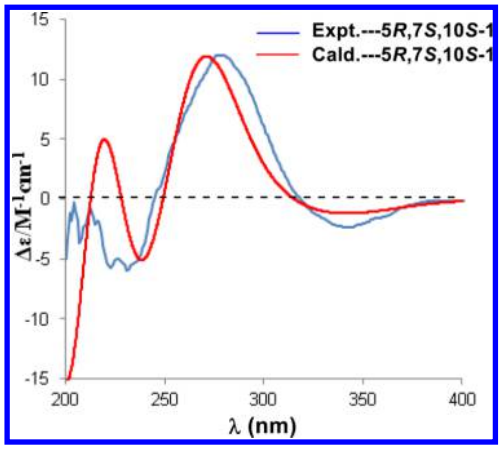

Figure 4. Experimental and calculated ECD curves of 5*R*,7*S*,10*S*-**1** in CH_3OH.

fornicatin A possessing a 3,4-*seco*-trinortriterpenoid skeleton.[21] However, the presence of a methyl and the absence of an oxymethylene indicated that a methyl at C-28 in **2** replaced the oxymethylene in fornicatin A, which was confirmed by the HMBC correlations (Figure 5) of H_3-28 (δ_H 1.46, s) and H_3-

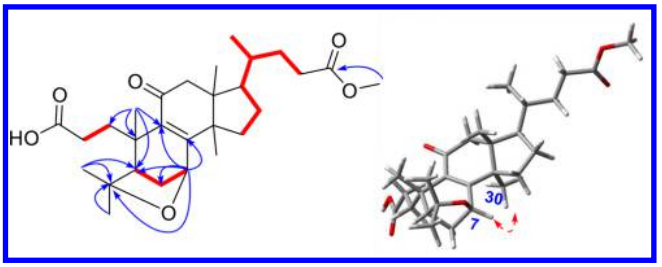

Figure 5. Selected HMBC (H → C), ^{1}H–^{1}H COSY (—), and ROESY (↔) correlations of **2**.

29 (δ_H 1.27, s) with C-4 (δ_C 84.4) and C-5 (δ_C 51.9); of H_3-19 (δ_H 1.58, s) with C-1, C-5, C-9 (δ_C 134.5), and C-10 (δ_C 41.3); of H-5 (δ_H 2.03, s) with C-4, C-6, C-7 (δ_C 73.1), C-10, and C-9; of H-7 with C-4. Moreover, the ^{1}H–^{1}H COSY correlations of H-5/H-6/H-7 also proved the deduction described above. In the HMBC spectrum, the methoxyl (δ_H 3.63, s) showed correlation with C-24 (δ_C 174.0), suggesting that OCH_3 was connected to C-24. Furthermore, the ROESY correlation of H_3-30/H-7 (Figure 5) suggested that the oxygen bridge between C-4 and C-7 was β-oriented. Thus, the structure of **2** was finally established.

To our knowledge, ganolearic acid A (**1**) represents the first example of lanostane-type triterpenoids with a 3/5/6/5-fused carbon skeleton. Fornicatin M (**2**) is a 3,4-*seco*-trinortriterpenoid possessing an oxygen bridge at C-4 and C-7. Analysis of their structures indicates that ganolearic acid A (**1**) and fornicatin M (**2**) might be derived from fornicatin D (**3**) (Scheme 1). The key carboncation intermediate (*i*) is formed from **3** under acidic conditions. When the long pair electrons of 7-OH attack C-4, fornicatin M (**2**) is generated by removal of Hydron. Additionally, a double bond between C-4 and C-5 is also produced by the deprotonation of C-5 (*ii*). Then, further protonation (*iii*), dehydration (*iv*), and an intermolecular proton transfer (*v*) lead to the formation of ganolearic acid A (**1**), with the loss of one molecule of acetone.

Furthermore, their anti-inflammatory activities were evaluated (positive control: L-NMMA), and the result showed that the inhibitory rate of compound **2** was 14.2 ± 2.0% for NO

DOI: 10.1021/acs.joc.8b01906
J. Org. Chem. XXXX, XXX, XXX–XXX

Scheme 1. Proposed Biogenetic Pathway of 1 and 2

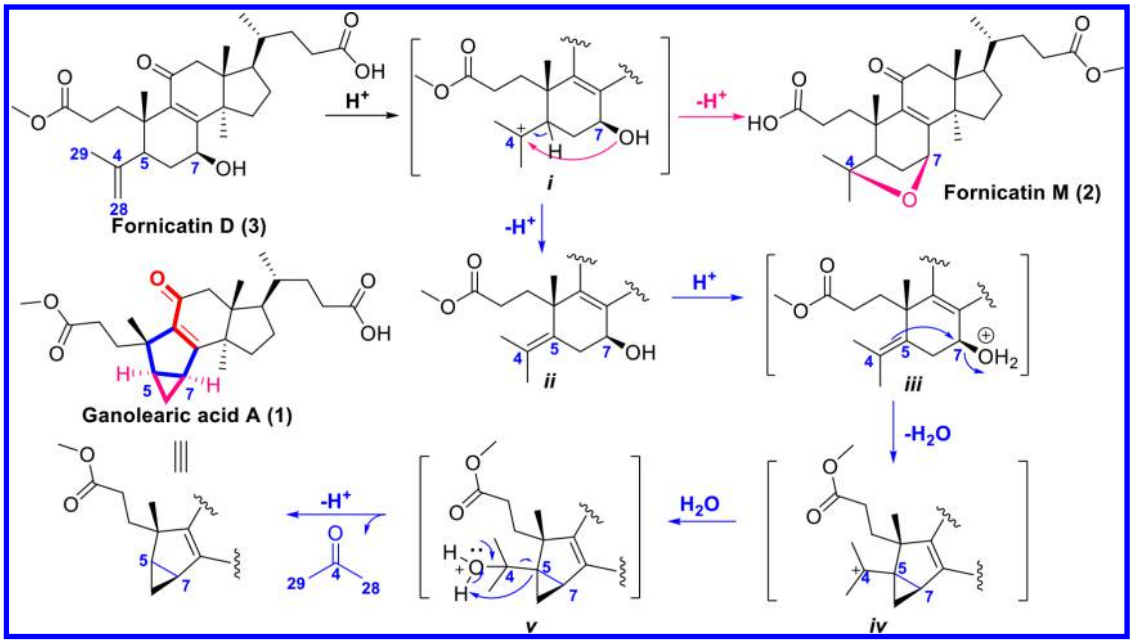

production induced by lipopolysacchrides (LPS) at a concentration of 50 μM.

CONCLUSION

In conclusion, a hexanorlanostane triterpenoid with a rare 3/5/6/5-fused tetracyclic skeleton, ganolearic acid A (**1**), was isolated from *G. cochlear* by a LC-UV/MS-guided method. A three-membered carbon motif of **1** is a unique structural change in lanostane-type triterpenoids. Our findings not only expand the chemical library of GMs but also provide plentiful structure models for bioactive study. *G. cochlear* showed various pharmacological effects, such as antitumor, liver protection, anti-diabetes, and antihypertension activities. Our previous phytochemcial investigation led to the isolation of a hexanorlanostane triterpenoid and a series of 3,4-*seco*-nortriterpenoid, as well as highly oxygenated lanostane triterpenoids from *G. cochlear* using a structure-guided method. Meanwhile, some of them showed hepatoprotective and cyctotoxic activities,[9,11] which indicates that GTs act an important role in explaining the effect of *G. cochlear* and it is worth discovering additional novel GTs from *G. cochlear*.

EXPERIMENTAL SECTION

General Experimental Procedures. UV spectra were recorded on a Shimadzu UV-2401PC spectrometer. Optical rotations were recorded on a Horiba SEPA-300 polarimeter. CD spectra were measured on a Chirascan instrument. Bruker AVIII-400 MHz and AVIII-800 MHz spectrometers (Bruker, Zurich, Switzerland) were used to determine NMR spectra. Chemical shifts (δ) were expressed in parts per million (ppm) with reference to the TMS resonance. The IR spectrum was recorded on a Bruker Tensor-27 instrument (KBr pellets). An API QSTAR Pulsar spectrometer was used to measure ESIMS, HRTOF-ESIMS, and UPLC-MS. An agilent 1100 and 1200 series instrument was used for high-performance liquid chromatography (HPLC) analysis. The specifications of the Agilent ZORBAX SB-C18 column were 5 μm, 9.6 mm × 250 mm.

Fungal Material. The fruiting bodies of *G. cochlear* (32 kg) were collected from Laos in July 2013. The specimen was identified by Prof. Liu Peigui and deposited at Kunming Institute of Botany, Chinese Academy of Science (voucher no. 13071501).

Extraction and Isolation. *Ganoderma cochlear* was extracted with EtOH (95%) under reflux three times (3 h per time). The ethanol extracts were concentrated, and the residue was suspended in H_2O. Then the H_2O layer was extracted with EtOAc. The EtOAc extracts were fractionated by macroporous resin (D-101; MeOH–H_2O, 50:50, 70:30, and 90:10, v/v) to obtain three fractions (fractions I–III). Fraction I (50 g) was further fractioned by an Rp-18 column with MeOH–H_2O as the mobile phase and gave 16 subfractions (Fr. I-1–Fr. I-16). Fr. I-2 was analyzed by HPLC to afford a chromatographic peak A (Figure S1A) with a λ_{max} at 285 nm. Furthermore, the UPLC-MS-IT-TOF method was used to analyze Fr. I-2 and determined the molecular formula of peak A to be $C_{25}H_{36}O_5Na$ and $C_{25}H_{35}O_5$ on the basis of the $[M + Na]^+$ ion (m/z 439.2453) in positive mode and the $[M - H]^-$ ion (m/z 415.2490) in negative mode (Figures S1), respectively. Consequently, Fr. I-2 (132 mg) was treated by HPLC on an Rp-18 column (CH_3CN/H_2O + 0.1% trifluoroacetic acid = 48%) to yield ganolearic acid A (Figure S1) (**1**, 2.5 mg, t_R = 21.5 min), fornicatin M (**2**, 12 mg, t_R = 22.7 min), and fornicatin D (**3**, 28 mg, t_R = 24.4 min).

*Ganolearic Acid A (**1**):* white powder (MeOH); $[\alpha]_D^{21}$ +49.4 (*c* 0.86, MeOH); UV (MeOH); λ_{max} (log ε) 279 (3.65), 217 (3.54), and 201 (3.73); IR (KBr) ν_{max} 3433, 2963, 2931, 1683, 1638, 1453, 1384, 1209, and 1142 cm^{-1}; for 1D NMR data, see Table 1; HRMS (ESI-TOF) m/z 415.2491 $[M - H]^-$ (calcd for $C_{25}H_{35}O_5$, 415.2490).

*Fornicatin M (**2**):* white powder (MeOH); $[\alpha]_D^{22}$ +46.6 (*c* 0.15, MeOH); UV (MeOH); λ_{max} (log ε) 265 (3.76), and 202 (3.47); IR (KBr) ν_{max} 3435, 2957, 1736, 1656, 1450, 1383, and 1207 cm^{-1}; for 1D NMR data, see Table 1; HRMS (ESI-TOF) m/z 473.2906 $[M - H]^-$ (calcd for $C_{28}H_{41}O_6$, 473.2909).

^{13}C NMR and ECD Calculations for 1. First, the selected conformations were optimized using the B3LYP/6-31G(d,p) method. Vibrational spectra of all optimized structures were calculated. Then ^{13}C NMR calculations were carried out at the levels of mPW1PW91/6-31G(d,p) with the gauge-independent atomic orbital method.[19] Meanwhile, considering the solvent effect, pyridine was used in the calculations process.[20] By subtracting the isotopic shifts for TMS calculated with the same methods,[19] the calculated ^{13}C NMR chemical shifts were obtained. Finally, on the basis of the Boltzmann distributions and the relative Gibbs free energies as weighting factors,[22] the ^{13}C NMR chemical shifts of each compound were expressed as the average values of the same atoms in the different conformers. Using the calculated chemical shifts δ_{calcd} to subtract the

DOI: 10.1021/acs.joc.8b01906
J. Org. Chem. XXXX, XXX, XXX–XXX

experimental chemical shifts δ_{exptl}, the difference ($\Delta\delta$) values were obtained.

The theoretical ECD calculations of compound **1** were performed using Gaussian 09.[20] Conformational analysis was carried out by providing the optimized conformation geometries and thermodynamic parameters of all conformations. Furthermore, time-dependent density functional theory at B3LYP/6-31G(d,p) level in MeOH with the polarized continuum model was used for the theoretical calculation of ECD. Meanwhile, the ECD spectra of compound **1** were obtained by weighing the Boltzmann distribution rate of each geometric conformation.

Anti-inflammatory Activity Assay.[23] Macrophage RAW264.7 cells were cultured in DMEM, which contained 10% FBS, 100 units/mL penicillin, and 100 μg/mL of streptomycin. Then 1 μg/mL LPS was added to stimulate RAW264.7 cells for NO production. Meanwhile, tested compounds were added to 96-well plates and were incubated overnight. At the same time, another two groups including a blank control group without tested compounds and positive control group (L-NMMA) were carried out. Then, the absorption values were determined at 570 nm. Cytotoxicity was tested by adding MTS in the remaining medium. The inhibition of NO production was calculated with the following formula: inhibition of NO production (%) = $(OD_{570\ nm\ blank} - OD_{570\ nm\ compounds})/OD_{570\ nm\ blank} \times 100\%$. IC_{50} (50% concentration of inhibition) values were determined based on the Reed & Muench method. All experiments were performed in triplicate.

■ ASSOCIATED CONTENT

Supporting Information

The Supporting Information is available free of charge on the ACS Publications website at DOI: 10.1021/acs.joc.8b01906.

1D NMR assignment of compounds **1** and **2**, NMR, MS spectra of **1** and **2**, CD and UV spectra, and computational data of compound **1**, together with experimental details (PDF)

■ AUTHOR INFORMATION

Corresponding Author

*Tel/fax: +86-871-65223327. E-mail: mhchiu@mail.kib.ac.cn.

ORCID

Ming-Hua Qiu: 0000-0001-9658-1636

Notes

The authors declare no competing financial interest.

■ ACKNOWLEDGMENTS

This study was financially supported by the National Natural Science Foundation of China (Nos. 21702209 and 81172940) and Foundation of State Key Laboratory of Phytochemistry and Plant Resources in West China (P2010-ZZ14).

■ REFERENCES

(1) Kubota, T.; Asaka, Y.; Miura, I.; Mori, H. Structures of ganoderic acid A and B, two new lanostane type bitter triterpenes from *Ganoderma lucidum* (FR.) KARST. *Helv. Chim. Acta* **1982**, *65*, 611−619.

(2) Zhang, J. J.; Ma, K.; Han, J. J.; Wang, K.; Chen, H. Y.; Bao, L.; Liu, L.; Xiong, W. P.; Zhang, Y. D.; Huang, Y.; Liu, H. W. Eight new triterpenoids with inhibitory activity against HMG-CoA reductase from the medical mushroom *Ganoderma leucocontextum* collected in Tibetan plateau. *Fitoterapia* **2018**, *130*, 79−88.

(3) Gill, B. S.; Navgeet; Mehra, R.; Kumar, V.; Kumar, S. Ganoderic acid, lanostanoid triterpene: a key player in apoptosis. *Invest. New Drugs* **2018**, *36*, 136−143.

(4) Martinez-Montemayor, M. M.; Acevedo, R. R.; Otero-Franqui, E.; Cubano, L. A.; Dharmawardhane, S. F. *Ganoderma lucidum* (Reishi) inhibits cancer cell growth and expression of key molecules in inflammatory breast cancer. *Nutr. Cancer* **2011**, *63*, 1085−1094.

(5) Ma, H. T.; Hsieh, J. F.; Chen, S. T. Anti-diabetic effects of *Ganoderma lucidum*. *Phytochemistry* **2015**, *114*, 109−113.

(6) Chen, H. Y.; Zhang, J. J.; Ren, J. W.; Wang, W. Z.; Xiong, W. P.; Zhang, Y. D.; Bao, L.; Liu, H. W. Triterpenes and meroterpenes with neuroprotective effects from *Ganoderma leucocontextum*. *Chem. Biodiversity* **2018**, *15*, e1700567.

(7) Baby, S.; Johnson, A. J.; Govindan, B. Secondary metabolites from *Ganoderma*. *Phytochemistry* **2015**, *114*, 66−101.

(8) Isaka, M.; Chinthanom, P.; Kongthong, S.; Srichomthong, K.; Choeyklin, R. Lanostane triterpenes from cultures of the Basidiomycete *Ganoderma orbiforme* BCC 22324. *Phytochemistry* **2013**, *87*, 133−139.

(9) Peng, X. R.; Liu, J. Q.; Wang, C. F.; Li, X. Y.; Shu, Y.; Zhou, L.; Qiu, M. H. Hepatoprotective effects of triterpenoids from *Ganoderma cochlear*. *J. Nat. Prod.* **2014**, *77*, 737−743.

(10) Wang, C. F.; Liu, J. Q.; Yan, Y. X.; Chen, J. C.; Lu, Y.; Guo, Y. H.; Qiu, M. H. Three new triterpenoids containing four-membered ring from the fruiting body of *Ganoderma sinense*. *Org. Lett.* **2010**, *12*, 1656−1659.

(11) Peng, X. R.; Wang, X.; Zhou, L.; Hou, B.; Zuo, Z. L.; Qiu, M. H. Ganocochlearic acid A, a rearranged hexanorlanostane triterpenoid, and cytotoxic triterpenoids from the fruiting bodies of *Ganoderma cochlear*. *RSC Adv.* **2015**, *5*, 95212−95222.

(12) Thao, N. P.; Luyen, B. T. T.; Lee, J. S.; Kim, J. H.; Dat, N. T.; Kim, Y. H. Inhibition potential of cycloartane-type glycosides from the roots of *Cimicifuga dahurica* against soluble epoxide hydrolase. *J. Nat. Prod.* **2017**, *80*, 1867−1875.

(13) Chen, J. Y.; Li, P. L.; Tang, X. L.; Wang, S. J.; Jiang, Y. T.; Shen, L.; Xu, B. M.; Shao, Y. L.; Li, G. Q. Cycloartane triterpenoids and their glycosides from the rhizomes of *Cimicifuga foetida*. *J. Nat. Prod.* **2014**, *77*, 1997−2005.

(14) Bao, N. M.; Nian, Y.; Zhu, G. L.; Wang, W. H.; Zhou, L.; Qiu, M. H. Cytotoxic 9,19-cycloartane triterpenes from the aerial parts of *Cimicifuga yunnanensis*. *Fitoterapia* **2014**, *99*, 191−197.

(15) Amen, Y. M.; Zhu, Q. C.; Afifi, M. S.; Halim, A. F.; Ashour, A.; Shimizu, K. New cytotoxic lanostanoid triterpenes from *Ganoderma* lingzhi. *Phytochem. Lett.* **2016**, *17*, 64−70.

(16) Lakornwong, W.; Kanokmedhakul, K.; Kanokmedhakul, S.; Kongsaeree, P.; Prabpai, S.; Sibounnavong, P.; Soytong, K. Triterpene lactones from clutures of *Ganoderma* sp. Km01. *J. Nat. Prod.* **2014**, *77*, 1545−1553.

(17) Huang, S. Z.; Ma, Q. Y.; Kong, F. D.; Guo, Z. K.; Cai, C. H.; Hu, L. L.; Zhou, L. M.; Wang, Q.; Dai, H. F.; Mei, W. L.; Zhao, Y. X. Lanostane-type triterpenoids from the fruiting body of *Ganoderma calidophilum*. *Phytochemistry* **2017**, *143*, 104−110.

(18) (a) Ditchfield, R. Self-consistent perturbation theory of diamagnetism. *Mol. Phys.* **1974**, *27*, 789−907. (b) McMichael Rohlfing, C.; Allen, L. C.; Ditchfield, R. Proton and carbon-13 chemical shifts: comparison between theory and experiment. *Chem. Phys.* **1984**, *87*, 9−15. (c) Wolinski, K.; Hinton, J. F.; Pulay, P. Efficient implementation of the gauge-independent atomic orbital method for NMR chemical shift calculations. *J. Am. Chem. Soc.* **1990**, *112*, 8251−8260.

(19) (a) Chaiken, J.; Gurnick, M.; McDonald, J. D. Statistical analysis of polyatomic quantum beats using the properties of random matrices. *J. Chem. Phys.* **1981**, *74*, 117−122. (b) Miertus, S.; Tomasi, J. Approximate evaluations of the electrostatic free energy and internal energy changes in solution processes. *Chem. Phys.* **1982**, *65*, 239−245. (c) Cossi, M.; Barone, V.; Cammi, R.; Tomasi, J. Ab initio study of solvated molecules: a new implementation of the polarizable continuum model. *Chem. Phys. Lett.* **1996**, *255*, 327−335.

(20) Frisch, M. J.; Trucks, G. W.; Schlegel, H. B.; Scuseria, G. E.; Robb, M. A.; Cheeseman, J. R.; Scalmani, G.; Barone, V.; Mennucci, B.; Petersson, G. A.; Nakatsuji, H.; Caricato, M.; Li, X.; Hratchian, H. P.; Izmaylov, A. F.; Bloino, J.; Zheng, G.; Sonnenberg, J. L.; Hada, M.; Ehara, M.; Toyota, K.; Fukuda, R.; Hasegawa, J.; Ishida, M.; Nakajima, T.; Honda, Y.; Kitao, O.; Nakai, H.; Vreven, T.;

DOI: 10.1021/acs.joc.8b01906
J. Org. Chem. XXXX, XXX, XXX−XXX

Montgomery, J. A., Jr.; Peralta, P. E.; Ogliaro, F.; Bearpark, M.; Heyd, J. J.; Brothers, E.; Kudin, K. N.; Staroverov, V. N.; Kobayashi, R.; Normand, J.; Raghavachari, K.; Rendell, A.; Burant, J. C.; Iyengar, S. S.; Tomasi, J.; Cossi, M.; Rega, N.; Millam, N. J.; Klene, M.; Knox, J. E.; Cross, J. B.; Bakken, V.; Adamo, C.; Jaramillo, J.; Gomperts, R.; Stratmann, R. E.; Yazyev, O.; Austin, A. J.; Cammi, R.; Pomelli, C.; Ochterski, J. W.; Martin, R. L.; Morokuma, K.; Zakrzewski, V. G.; Voth, G. A.; Salvador, P.; Dannenberg, J. J.; Dapprich, S.; Daniels, A. D.; Farkas, Ö.; Ortiz, J. V.; Cioslowski, J.; Fox, D. J. *Gaussian 09*, revision C.01; Gaussian, Inc.: Wallingford, CT, 2010.

(21) Niu, X. M.; Qiu, M. H.; Li, Z. R.; Lu, Y.; Cao, P.; Zheng, Q. T. Two novel 3,4-*seco*-trinorlanostane triterpenoids isolated from *Ganoderma fornicatum*. *Tetrahedron Lett.* **2004**, *45*, 2989−2993.

(22) Callam, C. S.; Singer, S. J.; Lowary, T. L.; Hadad, C. M. Computational analysis of the potential energy surfaces of glycerol in the gas and aqueous phases: effects of level of theory, basis set, and solvation on strongly intramolecularly hydrogen-bonded systems. *J. Am. Chem. Soc.* **2001**, *123*, 11743−11754.

(23) Chiu, C. P.; Liu, S. C.; Tang, C. H.; Chan, Y.; El-Shazly, M.; Lee, C. L.; Du, Y. C.; Wu, T. Y.; Chang, F. R.; Wu, Y.-C. Anti-inflammatory cerebrosides from cultivated *Cordyceps militaris*. *J. Agric. Food Chem.* **2016**, *64*, 1540−1548.

DOI: 10.1021/acs.joc.8b01906
J. Org. Chem. XXXX, XXX, XXX−XXX